

Generalized Nonlinear and Finsler Geometry for Robotics

Nathan D. Ratliff¹, Karl Van Wyk¹, Mandy Xie^{1,2}, Anqi Li^{1,3}, and Asif Muhammad Rana^{1,2}

Abstract—Robotics research has found numerous important applications of Riemannian geometry, despite the background mathematical material being strikingly challenging. This material is often remains inaccessible to roboticists, and despite many natural generalizations within the mathematical literature, there remain very few applications of modern highly-relevant geometric generalizations such as spray or Finsler geometry. This paper presents an entire re-derivation of generalized spray and Finsler geometries focusing on building the ideas from familiar concepts in advanced calculus and the calculus of variations. We focus on the pragmatic and calculable results and avoid the use of tensor notation to appeal to a broader audience. We have already used these derivations for important advances in our own work (for instance, geometric fabrics [1]); it is our hope that they will contribute to an increased understanding of these ideas within the robotics community and inspire future research into applications of generalized nonlinear, Finsler, and even Riemannian geometries.

I. INTRODUCTION

Riemannian geometry is in many ways fundamental to robotics. Robotic configuration spaces are most naturally modeled as a manifold [2], the classical mechanical dynamics of the robot is intimately linked to a Riemannian geometry [3], and natural gradient methods in machine learning. Riemannian geometry has made an impact on planning [4, 5].

However, Riemannian geometry, as a result of its obscure tensor notation, coordinate free descriptions, and focus on affine connections and curvature, remains exceedingly challenging to the general robotics audience. And importantly, there exists natural generalizations Riemannian geometry, such as spray and Finsler geometries, with undoubtably numerous impactful applications, that remain largely untouched by the community. If Riemannian geometry is challenging, these broader nonlinear geometries are impenetrable.

In studying the theoretical foundations of a modern line of reactive motion generation research, exemplified by Riemannian Motion Policies (RMPs)

[4] and the RMPflow algorithm [6], we recently found ourselves in need of understanding the fundamentals of generalized nonlinear geometry and Finsler geometry. Existing texts are extremely challenging, and we ultimately re-derived the core results rigorously from scratch, building from familiar concepts of advanced calculus [7] and the Calculus of Variations [8]. These results led to the development of a strong theoretically sound robust generalization of (RMPs) we call Geometric Fabrics [9], which inherit the intuitive design and modularity of RMPs while attaining stability and a form of geometric consistency that RMPs lacked. Geometric fabrics were a major advance in our understanding of modular reactive policies of this sort, and they have given us a powerful practical toolset for design. And none of that work would have been possible without a core understanding of these generalized nonlinear and Finsler geometries.

In this paper, we present our re-derivation of generalized nonlinear and Finsler geometry, providing intuition wherever possible. It is our hope that this work will inspire and enable many new applications of these geometries in robotics well beyond our initial exploration into geometric fabrics. Our contributions are:

- 1) We develop a class of generalized nonlinear geometries of paths characterized by homogeneous differential equations, focusing on their most fundamental form and their defining geometric path consistency properties.
- 2) We develop Finsler geometry from a Calculus of Variations perspective using notation familiar from advanced calculus and robotics (classical mechanics), using Riemannian geometry as an early example.
- 3) We prove the formal connection between dynamical systems derived from Finsler energies (including standard kinetic energy) and the corresponding nonlinear geometries of paths. This result extends the classical result of geometric mechanics connecting classical mechanics to Riemannian geometry.

¹All authors are with (or interned at) NVIDIA

²Georgia Tech

³University of Washington

- 4) Beyond generalized geometries, our derivations make Riemannian geometry, itself more accessible, and place it within the broader context of Finsler geometry.

Despite our novel treatment, this material is still challenging. It is our hope, however, that this presentation is at least accessible to many readers in ways the original mathematical material isn't. We hope this work bridges these powerful tools to a community of practitioners who will undoubtedly find important and influential applications.

A. A note on the literature

Many mathematical presentations of the ideas developed here exist (see [10] for a good introduction to Finsler geometry and [11] for an in-depth presentation of the generalization to spray geometry). However, the combination of abstract coordinate-free presentation and tensor notation for calculations, as well as their focus on highly theoretical ideas such as general nonlinear connections and global properties of curvature, make them highly inaccessible to most readers. We have found that practically much of the material around curvature is not used in robotic applications,¹ where path consistency and modeling of the resulting geodesic differential equations tend to be much more applicable (similar in areas of optimization on manifolds, such as those described in [12]). We, therefore, focus on deriving primarily the pre-curvature theory that relates more strongly to modeling differential equation behavior.

In the mathematical literature, generalizations of nonlinear geometries beyond Finsler tend to focus on what are called sprays and semi-sprays. We find these terms can be confusing for many readers as term spray pertains to more general differential equations with less structure and the term *semi*-spray pertains to the special class with *more* geo-

¹This is not to say it never will be—it's fundamental to applications in theoretical physics, especially in general relativity. A clear and accessible treatment of curvature would be in order should we find critical applications in robotics as well. These notions of curvature are more tricking in non-Riemannian geometry anyhow.

metric *path consistency*.² We, therefore, avoid these terms altogether, and call the more general class of geometries we derive in Section II *generalized nonlinear geometries* and focus solely on the case where geometries can be characterized based on their speed-independent *path consistency* (we sometimes refer to these as *geometries of paths*). This generalization fits well with the fundamental path-consistency properties of Finsler geometries (see Section III).

B. Notation and manifold concepts

In order to best serve a broad community of readers, we do not dwell on standard notions or definitions of manifolds and covariance. We instead follow what is done commonly in presentations of classical mechanics [13] and analytical dynamics [14] which is to assume we are working in a particular coordinate system. For those familiar with ideas around covariance [15, 16] we point out that the Euler-Lagrange equation which is used to derive many of the equations below is fundamentally covariant, which means practically that we can change coordinates as necessary to any curvilinear coordinate system and the fundamental behavior remains the same. The use of transform trees in systems modeling can also be used to attain covariance when the underlying equations themselves are not [6].

We avoid tensor notation altogether and instead derive all of our expressions using the notation of advanced calculus sticking to vector and matrix notations familiar to roboticists. This notation works well for our purposes since we avoid explicit discussions of curvature and connections, which are of interest primarily to mathematicians and theoretical physicists.

II. GENERALIZED NONLINEAR GEOMETRIES

A generalized nonlinear geometry is a second-order differential equation describing a smooth collection of paths. These paths are equivalence classes of trajectories all passing through the same points but with differing velocity profiles. A trajectory may speed up or slow down arbitrarily, but as long as its

²In mathematics, nonlinear connections and various definitions of curvature can be derived for a very broad class of second-order differential equation, so they call such differential equations *sprays* (the geometries can be characterized by their trajectory behavior at any point for the set of all initial valued problems defined by the tangent space at that point). A semi-spray, therefore, is just a particular subclass that is *more* geometrically consistent (trajectories pointing in the same direction follow the same path independent of initial speed).

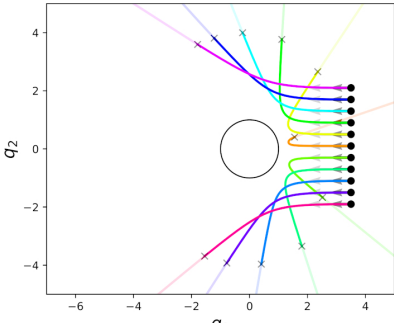


Fig. 1. Paths generated from particle motion initiated at different speeds. Faded paths indicate higher α and opaque paths indicate lower α .

geometric shape remains the same, it is part of the same path equivalence class. Colloquially, similar to how we can think of an arbitrarily second order differential equation as a collection of trajectories (its integral curves), we can think of the geometry as a collection of tubes. Each tube represents a path and contains multiple trajectories (infinitely many of them), the collection of all trajectories following that path with differing speed profiles (see Figure 1).

Concretely, two trajectories are said to be equivalent, and hence along the same path, if they are a *time reparameterization* away from one another. Given a trajectory with time index t denoted $\mathbf{x}_t = \mathbf{x}(t)$, a time reparameterization is a smooth, strictly monotonically increasing, nonlinear function $t : \mathbb{R} \rightarrow \mathbb{R}$ denoted $t(s)$ giving rise to a new time index s . the time reparameterization creates a new trajectory $\mathbf{x}_s = \mathbf{x}(t(s))$. Since, for a given s_0 and corresponding $t_0 = t(s_0)$, the points of the trajectories align

$$\mathbf{x}_s(s_0) = \mathbf{x}(t(s_0)) = \mathbf{x}_t(t_0), \quad (1)$$

and this relationship is a bijection,³ we can say that the two trajectories $\mathbf{x}_s(s)$ and $\mathbf{x}_t(t)$ follow the same path. Since $\frac{d}{ds}\mathbf{x}(t(s)) = \frac{d\mathbf{x}}{dt} \frac{dt}{ds}$ and $\frac{d^2}{ds^2}\mathbf{x}(t(s)) = \frac{d^2\mathbf{x}}{dt^2} \left(\frac{dt}{ds}\right)^2 + \frac{d\mathbf{x}}{dt} \frac{d^2t}{ds^2}$, we can see velocities and accelerations under the time reparameterization are linked to one another as

$$\begin{aligned} \dot{\mathbf{x}}_s &= \frac{dt}{ds} \dot{\mathbf{x}}_t \\ \ddot{\mathbf{x}}_s &= \left(\frac{dt}{ds}\right)^2 \ddot{\mathbf{x}}_t + \frac{d^2t}{ds^2} \dot{\mathbf{x}}_t, \end{aligned} \quad (2)$$

where notationally the dots are understood to be

³Formally, it is a diffeomorphism between coordinate charts of the same one-dimensional manifold of points.

time derivatives w.r.t. their respective time indices. E.g. $\dot{\mathbf{x}}_s = \frac{d\mathbf{x}_s}{ds}$, $\dot{\mathbf{x}}_t = \frac{d\mathbf{x}_t}{dt}$ and so forth. A smooth nonlinear geometry is defined by the collection of all time-reparameterization invariant paths in a space. For every point \mathbf{x} and speed-independent direction vector $\hat{\mathbf{v}}$, the nonlinear geometry defines a unique path emanating from that point following the specified initial direction $\hat{\mathbf{v}}$.

Denoting orthogonal projector projecting orthogonally to velocity as $\mathbf{P}_{\dot{\mathbf{x}}}^\perp = \mathbf{I} - \hat{\mathbf{x}}\hat{\mathbf{x}}^T$, the family of geometries we consider here are those characterized by a second-order differential equation of the form

$$\mathbf{P}_{\dot{\mathbf{x}}}^\perp [\ddot{\mathbf{x}} + \mathbf{h}_2(\mathbf{x}, \dot{\mathbf{x}})] = \mathbf{0}, \quad (3)$$

where $\mathbf{h}_2(\mathbf{x}, \dot{\mathbf{x}})$ is a smooth function that is *positively homogeneous of degree 2* (HD2) in velocities.⁴ We call equations of this form *geometric equations*.

Since the projector $\mathbf{P}_{\dot{\mathbf{x}}}^\perp$ is reduced rank, there is solution redundancy. We will see that this redundancy precisely describes the ability to arbitrarily speed up or slow down along a trajectory while sticking to the same path.

The interior equation in isolation

$$\ddot{\mathbf{x}} + \mathbf{h}_2(\mathbf{x}, \dot{\mathbf{x}}) = \mathbf{0} \quad (4)$$

is called the *generating equation* and is said to *generate* the geometry via its system of trajectories. Note that since $\mathbf{P}_{\dot{\mathbf{x}}}^\perp$ has null space spanned by $\dot{\mathbf{x}}$, solutions to the geometric equation are solutions to

$$\ddot{\mathbf{x}} + \mathbf{h}_2(\mathbf{x}, \dot{\mathbf{x}}) + \alpha(t)\dot{\mathbf{x}} = \mathbf{0} \quad (5)$$

where $\alpha : \mathbb{R} \rightarrow \mathbb{R}$ is a smooth function defining an acceleration along the direction of motion. We call this equation the *explicit form geometric equation*.

Theorem II.1. *All time reparameterizations of generating solutions are geometric solutions, and each geometric solution characterized by starting position \mathbf{x} and direction $\hat{\mathbf{v}}$ is a time reparameterization away from any generating solution with initial conditions $(\mathbf{x}, \gamma\hat{\mathbf{v}})$ for $\gamma > 0$.*

Proof. We first address reparameterization of generating solutions. Let $\mathbf{x}_s(s)$ be a generating solution trajectory and let $s(t)$ be an arbitrary time reparameterization

⁴Generally, a function $f(\mathbf{z})$ is said to be *positively homogeneous of degree k* (abbreviated HD k) if $f(\lambda\mathbf{z}) = \lambda^k f(\mathbf{z})$ for $\lambda \geq 0$ [17]. Homogeneity of degree 1 and 2 is used in the definitions below as well. In this case, \mathbf{h}_2 must be HD2, meaning $\mathbf{h}_2(\mathbf{x}, \lambda\dot{\mathbf{x}}) = \lambda^2 \mathbf{h}_2(\mathbf{x}, \dot{\mathbf{x}})$ for $\lambda > 0$.

terization. In terms of its inverse $t(s)$ (which always exists since $s(t)$ is strictly monotonically increasing by definition), by Equations 2 we have

$$\ddot{\mathbf{x}}_s + \mathbf{h}_2(\mathbf{x}_s, \dot{\mathbf{x}}_s) = \mathbf{0} \quad (6)$$

$$\Rightarrow \left(\frac{dt}{ds} \right)^2 \ddot{\mathbf{x}}_t + \frac{d^2t}{ds^2} \dot{\mathbf{x}}_t + \mathbf{h}_2(\mathbf{x}_t, \frac{dt}{ds} \dot{\mathbf{x}}_t) = \mathbf{0} \quad (7)$$

$$\Rightarrow \left(\frac{dt}{ds} \right)^2 [\ddot{\mathbf{x}}_t + \mathbf{h}_2(\mathbf{x}_t, \dot{\mathbf{x}}_t)] + \frac{d^2t}{ds^2} \dot{\mathbf{x}}_t = \mathbf{0} \quad (8)$$

$$\Rightarrow \ddot{\mathbf{x}}_t + \mathbf{h}_2(\mathbf{x}_t, \dot{\mathbf{x}}_t) + \alpha \dot{\mathbf{x}}_t = \mathbf{0}, \quad (9)$$

where $\alpha = \left(\frac{dt}{ds} \right)^{-2} \frac{d^2t}{ds^2}$. Thus, $\mathbf{x}_t(t)$ solves an explicit form geometric equation and is, therefore, a geometric solution.

Next, let $\mathbf{x}_s(s)$ be any solution to the geometric equation. Then at every point,

$$\ddot{\mathbf{x}}_s + \mathbf{h}_2(\mathbf{x}_s, \dot{\mathbf{x}}_s) + \alpha(s) \dot{\mathbf{x}}_s = \mathbf{0} \quad (10)$$

for some smooth function $\alpha(s)$ across the trajectory. Under a time reparameterization $s(t)$ we get the following equation in terms of \mathbf{x}_t

$$\begin{aligned} & \left(\frac{dt}{ds} \right)^2 \ddot{\mathbf{x}}_t + \frac{d^2t}{ds^2} \dot{\mathbf{x}}_t + \mathbf{h}_2(\mathbf{x}_t, \frac{dt}{ds} \dot{\mathbf{x}}_t) \\ & \quad + \alpha(s) \frac{dt}{ds} \dot{\mathbf{x}}_t = \mathbf{0} \\ \Rightarrow & \left(\frac{dt}{ds} \right)^2 [\ddot{\mathbf{x}}_t + \mathbf{h}_2(\mathbf{x}_t, \dot{\mathbf{x}}_t)] \\ & \quad + \left(\frac{d^2t}{ds^2} + \alpha(s) \frac{dt}{ds} \right) \dot{\mathbf{x}}_t = \mathbf{0}. \end{aligned}$$

Since $\frac{d^2t}{ds^2} + \alpha(s) \frac{dt}{ds} = 0$ is an ordinary second-order differential equation it has a unique solution for every initial condition $t(0), \frac{dt}{ds}(0)$. Under any of those solutions, the second term vanishes and we have $\ddot{\mathbf{x}}_t + \mathbf{h}_2(\mathbf{x}_t, \dot{\mathbf{x}}_t) = \mathbf{0}$ (since $\frac{dt}{ds} \neq 0$). Therefore, under such a time reparameterization, $\mathbf{x}_t(t)$ is a generating solution.

Moreover, since $\dot{\mathbf{x}}_s = \frac{dt}{ds} \dot{\mathbf{x}}_t$ the initial condition $\frac{dt}{ds}(0)$ defines the initial velocity $\dot{\mathbf{x}}_t(0) = \left(\frac{dt}{ds}(0) \right)^{-1} \dot{\mathbf{x}}_s(0)$ which uniquely defines the generating solution moving in direction $\hat{\mathbf{v}} = \hat{\mathbf{x}}_s(0)$. Since any initial velocity can be generated this way, every time reparameterization of this sort maps to a corresponding generating solution by initial conditions and every generating solution can be created by such a time reparameterization. Therefore, there is a bijection between time reparameterizations solving $\frac{d^2t}{ds^2} + \alpha(s) \frac{dt}{ds} = 0$ and generating solutions with initial conditions $(\mathbf{x}, \gamma \hat{\mathbf{v}})$. ■

The proof of the above theorem shows that any time reparameterization solving

$$\frac{d^2t}{ds^2} + \alpha(s) \frac{dt}{ds} = 0 \quad (11)$$

induces a generating solution. We are, therefore, free to choose the time reparameterization so that the generating solution's velocity matches the geometric solution's velocity at a given time (use the condition $\frac{dt}{ds}(0) = 1$ at the specific \bar{s} as the initial condition along with $t(\bar{s}) = \bar{s}$). With that mapping from s to corresponding generating solution whose velocity matches at $t(s)$, we can view the geometric solution as smoothly moving between generating solutions, using the redundant accelerations $\alpha(s) \dot{\mathbf{x}}_s$ to do so by speeding up and slowing down along the direction of motion.

To illustrate path consistency, we design a geometry, $\mathbf{h}_2(\mathbf{q}, \dot{\mathbf{q}})$, that naturally produces particle paths that avoid a circular object in coordinates, $\mathbf{q} \in \mathbb{R}^2$, as

$$\mathbf{h}_2(\mathbf{q}, \dot{\mathbf{q}}) = \lambda \|\dot{\mathbf{q}}\|^2 \partial_{\mathbf{q}} \psi(\phi(\mathbf{q})) \quad (12)$$

where $\phi(\mathbf{q})$ is a differentiable map that captures the distance to a circular object and $\lambda \in \mathbb{R}^+$ is a scaling gain. More specifically, $\phi(\mathbf{q}) = \frac{\|\mathbf{q} - \mathbf{q}_o\| - r}{r}$, where \mathbf{q}_o and r are the circle's center and radius, respectively. Furthermore, $\psi(\phi(\mathbf{q})) \in \mathbb{R}^+$ is a barrier potential function, $\psi(\phi(\mathbf{q})) = \frac{k}{\phi(\mathbf{q})^2}$, where $k \in \mathbb{R}^+$ is a scaling gain. Altogether, $\partial_{\mathbf{q}} \psi(\phi(\mathbf{q}))$ produces an increasing repulsive force as distance to the object decreases, and $\|\dot{\mathbf{q}}\|^2$ makes $\mathbf{h}_2(\mathbf{q}, \dot{\mathbf{q}})$ homogeneous of degree 2 in $\dot{\mathbf{q}}$. For this experiment, $\lambda = 0.7$, $k = 0.5$ for two scenarios: 1) $\alpha = 1.5$, and 2) $\alpha = 0.75$ for the initial conditions, $(\mathbf{q}_0, \alpha \dot{\mathbf{q}}_0)$. Eleven vertically spaced particles that follow the above geometry are initialized with the two different initial speeds. Traced paths at the two different speeds are overlayed as shown in Fig. 1. Noticeably, the paths generated are completely overlapping which confirms path consistency.

III. FINSLER GEOMETRY

Here, we derive a broad class of nonlinear geometries that arise from solutions to the Euler-Lagrange equation, known as Finsler geometries. We show that the generating equation also derives from the Euler-Lagrange equation, applied to an energy form of the geometric Lagrangian. These energy solutions are energy conserving and can thus be viewed as energy levels. Geometric solutions

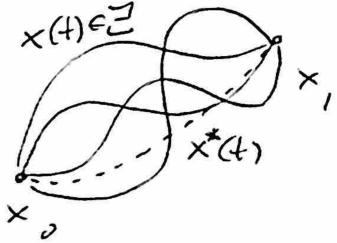


Fig. 2. A depiction of a Calculus of Variations problem. Solid lines are select trajectories $\mathbf{x}(t) \in \Xi$ between \mathbf{x}_0 and \mathbf{x}_1 from a smooth family of trajectories Ξ ; the dotted trajectory $\mathbf{x}^*(t)$ depicts an extremal trajectory that optimizes an objective functional.

to Finsler geometries, therefore, smoothly transition between these energy levels (generating solutions) by speeding up and slowing down along the direction of motion while remaining along the same common path.

A. The Euler-Lagrange equation

The Calculus of Variations [8] studies extremal trajectory problems. Given a function $\mathcal{L}(\mathbf{x}, \dot{\mathbf{x}})$ of position and velocity, known as a Lagrangian, and a class of smooth trajectories Ξ ranging between two end points \mathbf{x}_0 and \mathbf{x}_1 , we can ask which of those trajectories minimizes the “total Lagrangian” across the trajectory:

$$\min_{\mathbf{x}(t) \in \Xi} \int_0^T \mathcal{L}(\mathbf{x}, \dot{\mathbf{x}}) dt, \quad (13)$$

where T is understood to vary per trajectory based on its natural time interval length. The integral $A[\mathbf{x}] = \int \mathcal{L}(\mathbf{x}, \dot{\mathbf{x}}) dt$ is known as the Lagrangian’s *action*.

Figure 2 shows a simple (hypothetical) pictorial example. The dark trajectories depict possible candidates in Ξ and the dotted trajectory depicts the extremum. We won’t derive it here, but extremal solutions are characterized by solutions to the following boundary valued second-order differential equation:

$$\frac{d}{dt} \partial_{\dot{\mathbf{x}}} \mathcal{L} - \partial_{\mathbf{x}} \mathcal{L} = \mathbf{0} \quad \text{s.t.} \quad \begin{cases} \mathbf{x}(0) = \mathbf{x}_0 \\ \mathbf{x}(T) = \mathbf{x}_1 \end{cases} \quad (14)$$

This equation $\frac{d}{dt} \partial_{\dot{\mathbf{x}}} \mathcal{L} - \partial_{\mathbf{x}} \mathcal{L} = \mathbf{0}$ is important in its own right and is known as the Euler-Lagrange equation.⁵ By the theory of ordinary differential

⁵We write it in negated form here relative to the common expression from the Calculus of Variations [8] to match better with the equations of motion below, as we’ll see.

equations [18], this equation (second-order) has unique initial-value solutions when it is pointwise well-formed for $\dot{\mathbf{x}} \neq \mathbf{0}$ (we’ll see that this means its velocity Hessian $\partial^2 \dot{\mathbf{x}} \mathcal{L}$ is invertible for $\dot{\mathbf{x}} \neq \mathbf{0}$). This won’t be the case for Finsler structures (and we’ll get the solution redundancy characteristic of geometric equations from that), but it will be the case for the corresponding energy form generating equation.) This uniqueness of solution means that for any $(\mathbf{x}_0, \dot{\mathbf{x}}_0)$, we can play forward the Euler-Lagrange equation to generate a solution trajectory starting from that position and velocity. We can connect this solution back to the extremal problem by noting that every point \mathbf{x}_1 encountered along this initial-value solution is a possible end point and the solution to the initial-valued problem solves the boundary value problem with boundary constraints \mathbf{x}_0 and \mathbf{x}_1 . In other words, every subtrajectory of the initial-value solution is an extremal solution between its end points. Importantly, this enables us to consider the Euler-Lagrange equation in isolation and understand all of its solutions as extremal solutions of the action.

Expanding the time derivative brings the Euler-Lagrange equation to a more concrete form and clarifies its role as a second-order dynamical system:

$$\frac{d}{dt} \partial_{\dot{\mathbf{x}}} \mathcal{L} - \partial_{\mathbf{x}} \mathcal{L} = \mathbf{0} \quad (15)$$

$$\Rightarrow \partial_{\dot{\mathbf{x}}}^2 \mathcal{L} \ddot{\mathbf{x}} + \partial_{\dot{\mathbf{x}}\dot{\mathbf{x}}} \mathcal{L} \dot{\mathbf{x}} - \partial_{\mathbf{x}} \mathcal{L} = \mathbf{0} \quad (16)$$

$$\Rightarrow \mathbf{M}_{\mathcal{L}} \ddot{\mathbf{x}} + \mathbf{f}_{\mathcal{L}} = \mathbf{0}, \quad (17)$$

where $\mathbf{M}_{\mathcal{L}} = \partial_{\dot{\mathbf{x}}}^2 \mathcal{L}$ plays a role analogous to a mass matrix and $\mathbf{f}_{\mathcal{L}} = \partial_{\dot{\mathbf{x}}\dot{\mathbf{x}}} \mathcal{L} \dot{\mathbf{x}} - \partial_{\mathbf{x}} \mathcal{L}$ is a force-like object. Solutions to the Euler-Lagrange equation can be easily integrated forward from an initial position \mathbf{x} and velocity $\dot{\mathbf{x}}$ using the solved acceleration form $\ddot{\mathbf{x}} = -\mathbf{M}_{\mathcal{L}}^{-1} \mathbf{f}_{\mathcal{L}}$. Note that this solved form is only well-defined when $\mathbf{M}_{\mathcal{L}}$ is invertible as noted earlier. While here we consider $\mathbf{M}_{\mathcal{L}}$ and $\mathbf{f}_{\mathcal{L}}$ as merely analogous to mass and force, we will see that this analogy takes on a deeper, more concrete, meaning under Finsler geometry, where we require the Lagrangian to take on an intuitive form so that $\mathcal{L}(\mathbf{x}, \dot{\mathbf{x}})$, for fixed \mathbf{x} , becomes a squared norm like measure of velocities, giving it an interpretation of “length squared”. Under these particular Lagrangians, $\mathbf{M}_{\mathcal{L}}$ plays a role of mass, $\mathbf{f}_{\mathcal{L}}$ plays a role of force, and the equation $\ddot{\mathbf{x}} + \mathbf{M}_{\mathcal{L}}^{-1} \mathbf{f}_{\mathcal{L}} = \mathbf{0}$, or $\ddot{\mathbf{x}} + \mathbf{h}_2(\mathbf{x}, \dot{\mathbf{x}}) = \mathbf{0}$ with $\mathbf{h}_2 = \mathbf{M}_{\mathcal{L}}^{-1} \mathbf{f}_{\mathcal{L}}$ is a geometry generator.

B. Finsler structures

A *geometric Lagrangian* is a Lagrangian whose Euler-Lagrange equation can be expressed in the standard geometric form

$$P_{\dot{\mathbf{x}}}^\perp [\ddot{\mathbf{x}} + \mathbf{h}_2(\mathbf{x}, \dot{\mathbf{x}})] = \mathbf{0}, \quad (18)$$

where \mathbf{h}_2 is homogeneous of degree 2 in velocity (HD2). Recall that such degree 2 homogeneity implies an invariance to time-reparameterization (see Section II) of the geometric solutions characteristic of a geometry (solutions are velocity independent paths, not individual trajectories). A *Finsler structure* is a particular geometric Lagrangian \mathcal{L}_g with the following nice properties:

- 1) $\mathcal{L}_g(\mathbf{x}, \dot{\mathbf{x}}) \geq 0$ with equality if and only if $\dot{\mathbf{x}} = \mathbf{0}$.
- 2) \mathcal{L}_g is positively homogeneous (HD1) in $\dot{\mathbf{x}}$ so that $\mathcal{L}_g(\mathbf{x}, \lambda \dot{\mathbf{x}}) = \lambda \mathcal{L}_g(\mathbf{x}, \dot{\mathbf{x}})$ for $\lambda \geq 0$.
- 3) $\partial_{\dot{\mathbf{x}}}^2 \mathcal{L}_g$ is invertible when $\dot{\mathbf{x}} \neq \mathbf{0}$, where $\mathcal{L}_e = \frac{1}{2} \mathcal{L}_g^2$.

We call \mathcal{L}_e defined this way, the corresponding Finsler energy.

The positive homogeneity requirement means that the action functional is independent of time reparameterization. Recall that a time reparameterization is defined as $s = s(t)$ with $\dot{\mathbf{x}}_s = \frac{dt}{ds} \dot{\mathbf{x}}_t$, so the action function has the property

$$A[\mathbf{x}_s] = \int \mathcal{L}_g(\mathbf{x}_s, \dot{\mathbf{x}}_s) ds = \mathcal{L}_g \left(\mathbf{x}_t, \frac{dt}{dx} \dot{\mathbf{x}}_t \right) ds \quad (19)$$

$$= \int \mathcal{L}_g(\mathbf{x}_t, \dot{\mathbf{x}}_t) \frac{dt}{ds} ds \quad (20)$$

$$= \int \mathcal{L}_g(\mathbf{x}_t, \dot{\mathbf{x}}_t) dt = A[\mathbf{x}_t]. \quad (21)$$

This property, alone, suggests that solutions to the Euler-Lagrange equation of \mathcal{L}_g will be independent of time reparameterization. Theorem III.1 proves that conjecture. The speed independence of this action functional, in conjunction with the conditions of a Finsler structure listed above, also suggests we can view the Finsler structure \mathcal{L}_g as a generalized *length element*. The action functional is, therefore, a generalized arc-length integral.

Each Finsler structure \mathcal{L}_g has an associated *energy form* $\mathcal{L}_e = \frac{1}{2} \mathcal{L}_g^2$. Since \mathcal{L}_g is HD1, $\mathcal{L}_e(\mathbf{x}, \lambda \dot{\mathbf{x}}) = \frac{1}{2} (\mathcal{L}_g(\mathbf{x}, \lambda \dot{\mathbf{x}}))^2 = \lambda^2 \frac{1}{2} (\mathcal{L}_g(\mathbf{x}, \dot{\mathbf{x}}))^2 = \lambda^2 \mathcal{L}_e(\mathbf{x}, \dot{\mathbf{x}})$, so the Finsler energy \mathcal{L}_e is positively homogeneous of degree 2 (HD2). A useful property homogeneity is given by Euler's theorem on homo-

geneous functions [17], which states that if $\mathcal{L}(\mathbf{x}, \dot{\mathbf{x}})$ is homogeneous of degree k in $\dot{\mathbf{x}}$, then

$$\mathcal{H}_{\mathcal{L}} = \partial_{\dot{\mathbf{x}}} \mathcal{L}^T \dot{\mathbf{x}} - \mathcal{L} = (k-1) \mathcal{L}. \quad (22)$$

In the case of the energy Lagrangian $\mathcal{L}_e = \frac{1}{2} \mathcal{L}_g^2$, we have $k = 2$, so

$$\mathcal{H}_{\mathcal{L}_e} = (k-1) \mathcal{L}_e = \mathcal{L}_e. \quad (23)$$

The equations of motion under the Energy Lagrangian \mathcal{L}_e , which we call the energy equations, are

$$\partial_{\dot{\mathbf{x}}}^2 \mathcal{L}_e \ddot{\mathbf{x}} + \partial_{\dot{\mathbf{x}}\dot{\mathbf{x}}} \mathcal{L}_e \dot{\mathbf{x}} - \partial_x \mathcal{L}_e = \mathbf{0} \quad (24)$$

$$\Leftrightarrow \mathbf{M}_e \ddot{\mathbf{x}} + \mathbf{f}_e = \mathbf{0}, \quad (25)$$

where $\mathbf{M}_e = \partial_{\dot{\mathbf{x}}}^2 \mathcal{L}_e$ and $\mathbf{f}_e = \partial_{\dot{\mathbf{x}}\dot{\mathbf{x}}} \mathcal{L}_e \dot{\mathbf{x}} - \partial_x \mathcal{L}_e$. Since these equations are known to conserve \mathcal{H}_e , and in this case $\mathcal{H}_e = \mathcal{L}_e$, we see that this Finsler energy is conserved). \mathcal{L}_e is often referred to as the *energy* of the system, and \mathbf{M}_e is its *energy tensor*.

Note that the third requirement on Finsler structures given above is actually a requirement on the Finsler *energy* \mathcal{L}_e . It ensures that \mathbf{M}_e is invertable by definition when $\dot{\mathbf{x}} = \mathbf{0}$. The equations of motion $\mathbf{M}_e \ddot{\mathbf{x}} + \mathbf{f}_e = \mathbf{0}$, therefore, can always be solved to give a unique acceleration form

$$\ddot{\mathbf{x}} + \mathbf{M}_e^{-1} \mathbf{f}_e = \mathbf{0}. \quad (26)$$

This equation is known as the *geodesic equation*, and we will see that it acts as a generator for the geometry expressed by the \mathcal{L}_g 's equations of motion.

Without proving it here, we note that taking derivatives in $\dot{\mathbf{x}}$ reduces \mathcal{L}_e 's homogeneity by 1 (a general property of homogeneous functions). Therefore, examining \mathbf{f}_e , we see

$$\mathbf{f}_e = \partial_{\dot{\mathbf{x}}\dot{\mathbf{x}}} \mathcal{L}_e \dot{\mathbf{x}} - \partial_x \mathcal{L}_e, \quad (27)$$

for which $\partial_x \mathcal{L}_e$ is HD2 already, and $\dot{\mathbf{x}}$ multiplies the HD1 $\partial_{\dot{\mathbf{x}}\dot{\mathbf{x}}} \mathcal{L}_e$ making $\partial_{\dot{\mathbf{x}}\dot{\mathbf{x}}} \mathcal{L}_e \dot{\mathbf{x}}$ HD2 as well. So \mathbf{f}_e is HD2 in its entirety. Moreover, $\mathbf{M}_e = \partial_{\dot{\mathbf{x}}}^2 \mathcal{L}_e$ has two derivatives so it is HD0 (i.e. $\mathbf{M}_e(\mathbf{x}, \lambda \dot{\mathbf{x}}) = \mathbf{M}_e(\mathbf{x}, \dot{\mathbf{x}})$, meaning the energy tensor is independent of the scale of the velocity and, therefore, depends only on $\dot{\mathbf{x}}$'s directionality). That means $\mathbf{h}_2(\mathbf{x}, \dot{\mathbf{x}}) = \mathbf{M}_e^{-1} \mathbf{f}_e$ is HD2, making the geodesic equation $\ddot{\mathbf{x}} + \mathbf{M}_e^{-1} \mathbf{f}_e = \mathbf{0}$ a generating equation, with associated geometric equation

$$P_{\dot{\mathbf{x}}}^\perp [\ddot{\mathbf{x}} + \mathbf{M}_e^{-1} \mathbf{f}_e] = \mathbf{0}. \quad (28)$$

The following theorem shows that this geometry

is precisely that characterized by \mathcal{L}_g 's equations of motion. We denote the geometric equations of motion by $\mathbf{M}_g \ddot{\mathbf{x}} + \mathbf{f}_g = \mathbf{0}$ where $\mathbf{M}_g = \partial_{\dot{\mathbf{x}}}^2 \mathcal{L}_g$ and $\mathbf{f}_g = \partial_{\dot{\mathbf{x}}\dot{\mathbf{x}}} \mathcal{L}_g - \partial_{\dot{\mathbf{x}}} \mathcal{L}_g$ for Finsler structure \mathcal{L}_g . In this case, \mathbf{M}_g is reduced rank, as we will see, so we can't solve for a unique acceleration. Instead, the redundancy is precisely that expressed by the geometric equation.

Theorem III.1. *Let \mathcal{L}_g be a Finsler structure with energy form $\mathcal{L}_e = \frac{1}{2} \mathcal{L}_g^2$. Then the energy equations $\mathbf{M}_e \ddot{\mathbf{x}} + \mathbf{f}_e = \mathbf{0}$ is a generating equation with the associated geometry given by the geometric equations $\mathbf{M}_g \ddot{\mathbf{x}} + \mathbf{f}_g = \mathbf{0}$.*

Proof. We already observed that $\mathbf{h}_2(\mathbf{x}, \dot{\mathbf{x}}) = \mathbf{M}_e^{-1} \mathbf{f}_e$ is homogeneous of degree 2, so $\ddot{\mathbf{x}} + \mathbf{h}_2(\mathbf{x}, \dot{\mathbf{x}}) = \mathbf{0}$ is a generating equation where it is (uniquely) defined. Since \mathbf{M}_e is invertible by definition when $\dot{\mathbf{x}} \neq \mathbf{0}$, it is only undefined for $\dot{\mathbf{x}} = \mathbf{0}$. But for $\dot{\mathbf{x}} = \mathbf{0}$, solutions to $\mathbf{M}_e \ddot{\mathbf{x}} + \mathbf{f}_e = \mathbf{0}$ are stationary point trajectories ($\ddot{\mathbf{x}} = \mathbf{0}$) since \mathbf{f}_e is homogeneous. Therefore, defining $\mathbf{h}_2(\mathbf{x}, \mathbf{0}) = \mathbf{0}$ creates matching limiting behavior (independent of the characteristic properties of generating equations, which characterize geometrically consistent generating trajectories for $\dot{\mathbf{x}} \neq \mathbf{0}$), so $\ddot{\mathbf{x}} + \mathbf{h}_2(\mathbf{x}, \dot{\mathbf{x}}) = \mathbf{0}$ is a generating equation with solutions consistent with $\mathbf{M}_e \ddot{\mathbf{x}} + \mathbf{f}_e = \mathbf{0}$.

To show $\mathbf{M}_g \ddot{\mathbf{x}} + \mathbf{f}_g = \mathbf{0}$ is a geometric equation, we calculate explicit expressions for \mathbf{M}_g and \mathbf{f}_g . $\mathcal{L}_e = \frac{1}{2} \mathcal{L}_g^2$, so $\mathcal{L}_g = (2\mathcal{L}_e)^{\frac{1}{2}}$. Therefore,

$$\begin{aligned} \mathbf{M}_g &= \partial_{\dot{\mathbf{x}}}^2 \mathcal{L}_g = \sqrt{2} \partial_{\dot{\mathbf{x}}} \left[\partial_{\dot{\mathbf{x}}} \mathcal{L}_e^{\frac{1}{2}} \right] = \sqrt{2} \mathcal{L}_e^{-\frac{1}{2}} \partial_{\dot{\mathbf{x}}} \mathcal{L}_e \\ &= \frac{\sqrt{2}}{2} \left[\left(-\frac{1}{2} \right) \mathcal{L}_e^{-\frac{1}{2}-1} \partial_{\dot{\mathbf{x}}} \mathcal{L}_e \partial_{\dot{\mathbf{x}}} \mathcal{L}_e^T + \mathcal{L}_e^{-\frac{1}{2}} \partial_{\dot{\mathbf{x}}}^2 \mathcal{L}_e \right] \\ &= \frac{1}{(2\mathcal{L}_e)^{\frac{1}{2}}} \left[\partial_{\dot{\mathbf{x}}}^2 \mathcal{L}_e - \frac{1}{2\mathcal{L}_e} \partial_{\dot{\mathbf{x}}} \mathcal{L}_e \partial_{\dot{\mathbf{x}}} \mathcal{L}_e^T \right] \\ &= \frac{1}{\mathcal{L}_g} \left[\mathbf{M}_e - \frac{\mathbf{p}_e \mathbf{p}_e^T}{\mathbf{p}_e^T \mathbf{M}_e^{-1} \mathbf{p}_e} \right], \end{aligned}$$

where we use $\mathbf{M}_e = \partial_{\dot{\mathbf{x}}}^2 \mathcal{L}_e$ and denote $\mathbf{p}_e = \partial_{\dot{\mathbf{x}}} \mathcal{L}_e$ (this quantity is called the generalized momentum and has a recurring role in Finsler theory). We also use the following identity, which we will prove in Lemma III.2:

$$\mathcal{L}_e = \frac{1}{2} \mathbf{p}_e^T \mathbf{M}_e^{-1} \mathbf{p}_e. \quad (29)$$

Denoting $\mathbf{R}_{\dot{\mathbf{x}}} = \mathbf{M}_e - \frac{\mathbf{p}_e \mathbf{p}_e^T}{\mathbf{p}_e^T \mathbf{M}_e^{-1} \mathbf{p}_e}$ and noting $\mathbf{p}_e = \mathbf{M}_e \dot{\mathbf{x}}$ (also proved in Lemma III.2), we see that

$\mathbf{M}_g = \frac{1}{\mathcal{L}_g} \mathbf{R}_{\dot{\mathbf{x}}}$ is a reduced rank matrix with null space spanned by $\dot{\mathbf{x}}$

$$\mathbf{R}_{\dot{\mathbf{x}}} \dot{\mathbf{x}} = \left(\mathbf{M}_e - \frac{\mathbf{p}_e \mathbf{p}_e^T}{\mathbf{p}_e^T \mathbf{M}_e^{-1} \mathbf{p}_e} \right) \mathbf{M}_e^{-1} \mathbf{p}_e \quad (30)$$

$$= \mathbf{M}_e \mathbf{M}_e^{-1} \mathbf{p}_e - \frac{\mathbf{p}_e (\mathbf{p}_e^T \mathbf{M}_e^{-1} \mathbf{p}_e)}{\mathbf{p}_e^T \mathbf{M}_e^{-1} \mathbf{p}_e} \quad (31)$$

$$= \mathbf{p}_e - \mathbf{p}_e = \mathbf{0}. \quad (32)$$

Using a calculation analogous to that which we used for Equation 29 we get

$$\partial_{\dot{\mathbf{x}}\dot{\mathbf{x}}} \mathcal{L}_g = \frac{1}{\mathcal{L}_g} \left[\partial_{\dot{\mathbf{x}}\dot{\mathbf{x}}} \mathcal{L}_e - \frac{1}{2\mathcal{L}_e} \partial_{\dot{\mathbf{x}}} \mathcal{L}_e \partial_{\dot{\mathbf{x}}} \mathcal{L}_e^T \right], \quad (33)$$

and separately,

$$\partial_{\dot{\mathbf{x}}} \mathcal{L}_g = \partial_{\dot{\mathbf{x}}} (2\mathcal{L}_e)^{\frac{1}{2}} = \frac{\sqrt{2}}{2} \mathcal{L}_e^{-\frac{1}{2}} \partial_{\dot{\mathbf{x}}} \mathcal{L}_e = \frac{1}{\mathcal{L}_g} \partial_{\dot{\mathbf{x}}} \mathcal{L}_e, \quad (34)$$

so combining we get

$$\begin{aligned} \mathbf{f}_g &= \partial_{\dot{\mathbf{x}}\dot{\mathbf{x}}} \mathcal{L}_g \dot{\mathbf{x}} - \partial_{\dot{\mathbf{x}}} \mathcal{L}_g \\ &= \frac{1}{\mathcal{L}_g} \left[(\partial_{\dot{\mathbf{x}}\dot{\mathbf{x}}} \mathcal{L}_e \dot{\mathbf{x}} - \partial_{\dot{\mathbf{x}}} \mathcal{L}_e) - \frac{1}{2\mathcal{L}_e} \partial_{\dot{\mathbf{x}}} \mathcal{L}_e \partial_{\dot{\mathbf{x}}} \mathcal{L}_e^T \dot{\mathbf{x}} \right] \\ &= \frac{1}{\mathcal{L}_g} \left[\mathbf{f}_e - \frac{1}{2\mathcal{L}_e} \partial_{\dot{\mathbf{x}}} \mathcal{L}_e \partial_{\dot{\mathbf{x}}} \mathcal{L}_e^T \dot{\mathbf{x}} \right]. \end{aligned}$$

We first show that $\dot{\mathbf{x}}^T \mathbf{f}_g = \mathbf{0}$ (i.e. \mathbf{f}_g is orthogonal to $\dot{\mathbf{x}}$) and then use that insight to derive an explicit projected expression for \mathbf{f}_g :

$$\dot{\mathbf{x}}^T \mathbf{f}_g = \frac{1}{\mathcal{L}_g} \left[\dot{\mathbf{x}}^T \mathbf{f}_e - \frac{1}{2\mathcal{L}_e} \dot{\mathbf{x}}^T \partial_{\dot{\mathbf{x}}} \mathcal{L}_e \partial_{\dot{\mathbf{x}}} \mathcal{L}_e^T \dot{\mathbf{x}} \right] \quad (34)$$

$$\begin{aligned} &= \frac{1}{\mathcal{L}_g} \left[\dot{\mathbf{x}}^T (\partial_{\dot{\mathbf{x}}\dot{\mathbf{x}}} \mathcal{L}_e \dot{\mathbf{x}} - \partial_{\dot{\mathbf{x}}} \mathcal{L}_e) \right. \\ &\quad \left. - \frac{\frac{1}{2} \dot{\mathbf{x}}^T \partial_{\dot{\mathbf{x}}} \mathcal{L}_e}{\mathcal{L}_e} \partial_{\dot{\mathbf{x}}} \mathcal{L}_e^T \dot{\mathbf{x}} \right]. \end{aligned} \quad (35)$$

From Lemma III.2 we also get $\mathcal{L}_e = \frac{1}{2} \mathbf{p}_e^T \dot{\mathbf{x}} = \frac{1}{2} \partial_{\dot{\mathbf{x}}} \mathcal{L}_e^T \dot{\mathbf{x}}$, so the expression reduces to

$$\dot{\mathbf{x}}^T \mathbf{f}_g = \frac{1}{\mathcal{L}_g} [\dot{\mathbf{x}}^T \partial_{\dot{\mathbf{x}}\dot{\mathbf{x}}} \mathcal{L}_e \dot{\mathbf{x}} - 2\partial_{\dot{\mathbf{x}}} \mathcal{L}_e^T \dot{\mathbf{x}}]. \quad (36)$$

Finally,

$$\dot{\mathbf{x}}^T \partial_{\dot{\mathbf{x}}\dot{\mathbf{x}}} \dot{\mathbf{x}} - 2\partial_{\dot{\mathbf{x}}} \mathcal{L}_e^T \dot{\mathbf{x}} \quad (37)$$

$$= (\dot{\mathbf{x}}^T \partial_{\dot{\mathbf{x}}} (\partial_{\dot{\mathbf{x}}} \mathcal{L}_e) - 2\partial_{\dot{\mathbf{x}}} \mathcal{L}_e) \dot{\mathbf{x}} \quad (38)$$

$$= \partial_{\dot{\mathbf{x}}} (\dot{\mathbf{x}}^T \partial_{\dot{\mathbf{x}}} \mathcal{L}_e - 2\mathcal{L}_e) \dot{\mathbf{x}} \quad (39)$$

$$= \partial_{\dot{\mathbf{x}}} (2\mathcal{L}_e - 2\mathcal{L}_e) \dot{\mathbf{x}} = \mathbf{0}, \quad (40)$$

again since $\mathcal{L}_e = \frac{1}{2} \partial_{\dot{\mathbf{x}}} \mathcal{L}_e^T \dot{\mathbf{x}}$ by Lemma III.2. Therefore, $\dot{\mathbf{x}}^T \mathbf{f}_g = \mathbf{0}$.

Since \mathbf{f}_g is orthogonal to $\dot{\mathbf{x}}$ and $\mathbf{f}_g =$

$\frac{1}{\mathcal{L}_g} [\mathbf{f}_e - \alpha \mathbf{p}_e]$ where $\mathbf{p}_e = \partial_{\dot{\mathbf{x}}} \mathcal{L}_e$ and $\alpha = \frac{1}{2\mathcal{L}_e} \partial_{\dot{\mathbf{x}}} \mathcal{L}_e^T \dot{\mathbf{x}}$, α must be precisely the coefficient on \mathbf{p}_e needed to remove the component of \mathbf{f}_e along $\dot{\mathbf{x}}$. Explicitly, α must satisfy $\dot{\mathbf{x}}^T [\mathbf{f}_e - \alpha \mathbf{p}_e] = 0$, which means

$$\alpha = \frac{\dot{\mathbf{x}}^T \mathbf{f}_e}{\dot{\mathbf{x}}^T \mathbf{p}_e} \quad (41)$$

is another expression for α . That means

$$\mathbf{f}_g = \frac{1}{\mathcal{L}_g} [\mathbf{f}_e - \alpha \mathbf{p}_e] = \frac{1}{\mathcal{L}_g} \left[\mathbf{f}_e - \left(\frac{\dot{\mathbf{x}}^T \mathbf{f}_e}{\dot{\mathbf{x}}^T \mathbf{p}_e} \right) \mathbf{p}_e \right] \quad (42)$$

$$= \frac{1}{\mathcal{L}_g} \left[\mathbf{I} - \frac{\mathbf{p}_e \dot{\mathbf{x}}^T}{\dot{\mathbf{x}}^T \mathbf{p}_e} \right] \mathbf{f}_e. \quad (43)$$

Noting again that $\mathbf{p}_e = \mathbf{M}_e \dot{\mathbf{x}}$ (see Lemma III.2), we have

$$\mathbf{f}_g = \frac{1}{\mathcal{L}_g} \left[\mathbf{I} - \frac{\mathbf{M}_e \dot{\mathbf{x}} \dot{\mathbf{x}}^T}{\dot{\mathbf{x}}^T \mathbf{M}_e \dot{\mathbf{x}}} \right] \mathbf{f}_e \quad (44)$$

$$= \frac{1}{\mathcal{L}_g} \mathbf{M}_e \left[\mathbf{M}_e^{-1} - \frac{\dot{\mathbf{x}} \dot{\mathbf{x}}^T}{\dot{\mathbf{x}}^T \mathbf{M}_e \dot{\mathbf{x}}} \right] \mathbf{f}_e \quad (45)$$

$$= \frac{1}{\mathcal{L}_g} \mathbf{M}_e \mathbf{R}_{\mathbf{p}_e} \mathbf{f}_e, \quad (46)$$

where

$$\mathbf{R}_{\mathbf{p}_e} = \mathbf{M}_e^{-1} - \frac{\dot{\mathbf{x}} \dot{\mathbf{x}}^T}{\dot{\mathbf{x}}^T \mathbf{M}_e \dot{\mathbf{x}}} \quad (47)$$

is a reduced rank matrix analogous to $\mathbf{R}_{\dot{\mathbf{x}}}$, with null space spanned by $\mathbf{p}_e = \mathbf{M}_e \dot{\mathbf{x}}$.

Combining all of these expressions so far, we get geometric equations of motion

$$\mathbf{M}_g \ddot{\mathbf{x}} + \mathbf{f}_g = \frac{1}{\mathcal{L}_g} \mathbf{R}_{\dot{\mathbf{x}}} \ddot{\mathbf{x}} + \frac{1}{\mathcal{L}_g} \mathbf{M}_e \mathbf{R}_{\mathbf{p}_e} \mathbf{f}_e = \mathbf{0}. \quad (48)$$

However, $\mathbf{R}_{\dot{\mathbf{x}}}$ and $\mathbf{R}_{\mathbf{p}_e}$ are related by the identity $\mathbf{M}_e \mathbf{R}_{\mathbf{p}_e} \mathbf{M}_e = \mathbf{R}_{\dot{\mathbf{x}}}$ since

$$\mathbf{R}_{\dot{\mathbf{x}}} = \mathbf{M}_e - \frac{\mathbf{p}_e \mathbf{p}_e^T}{\mathbf{p}_e^T \mathbf{M}_e^{-1} \mathbf{p}_e} \quad (49)$$

$$= \mathbf{M}_e - \frac{\mathbf{M}_e \dot{\mathbf{x}} \dot{\mathbf{x}}^T \mathbf{M}_e}{(\mathbf{M}_e \dot{\mathbf{x}})^T \mathbf{M}_e^{-1} (\mathbf{M}_e \dot{\mathbf{x}})} \quad (50)$$

$$= \mathbf{M}_e \left[\mathbf{M}_e^{-1} - \frac{\dot{\mathbf{x}} \dot{\mathbf{x}}^T}{\dot{\mathbf{x}}^T \mathbf{M}_e \dot{\mathbf{x}}} \right] \mathbf{M}_e \quad (51)$$

$$= \mathbf{M}_e \mathbf{R}_{\mathbf{p}_e} \mathbf{M}_e. \quad (52)$$

Therefore, the geometric equations of motion can

be expressed

$$\frac{1}{\mathcal{L}_g} \mathbf{M}_e \mathbf{R}_{\mathbf{p}_e} \mathbf{M}_e \ddot{\mathbf{x}} + \frac{1}{\mathcal{L}_g} \mathbf{M}_e \mathbb{R}_{\mathbf{p}_e} \mathbf{f}_e = \mathbf{0} \quad (53)$$

$$\Rightarrow \frac{1}{\mathcal{L}_g} \mathbf{M}_e \mathbf{R}_{\mathbf{p}_e} [\mathbf{M}_e \ddot{\mathbf{x}} + \mathbf{f}_e] = \mathbf{0} \quad (54)$$

$$\text{or } \mathbf{P}_{\mathbf{p}_e}^\perp [\mathbf{M}_e \ddot{\mathbf{x}} + \mathbf{f}_e] = \mathbf{0}, \quad (55)$$

where $\mathbf{P}_{\mathbf{p}_e}^\perp$ is an orthogonal projector with null space \mathbf{p}_e (any matrix with \mathbf{p}_e spanning its null space would express the same equation). Solutions to this equation are exactly those for which $\mathbf{M}_e \ddot{\mathbf{x}} + \mathbf{f}_e$ lies along the null space \mathbf{p}_e , so they can be expressed as solutions to the unprojected equation

$$\mathbf{M}_e \ddot{\mathbf{x}} + \mathbf{f}_e + \alpha \mathbf{p}_e = \mathbf{0} \quad (56)$$

for any $\alpha \in \mathbb{R}$. Since $\mathbf{p}_e = \mathbf{M}_e \dot{\mathbf{x}}$ by Lemma III.2, those solutions also solve

$$\mathbf{M}_e \ddot{\mathbf{x}} + \mathbf{f}_e + \alpha \mathbf{M}_e \dot{\mathbf{x}} = \mathbf{0} \quad (57)$$

$$\Rightarrow \ddot{\mathbf{x}} + \mathbf{M}_e^{-1} \mathbf{f}_e + \alpha \dot{\mathbf{x}} = \mathbf{0} \quad (58)$$

for any $\alpha \in \mathbb{R}$, which are exactly the solutions to

$$\mathbf{P}_{\dot{\mathbf{x}}}^\perp [\ddot{\mathbf{x}} + \mathbf{M}_e^{-1} \mathbf{f}_e] = \mathbf{0}, \quad (59)$$

where $\mathbf{P}_{\dot{\mathbf{x}}}^\perp$ is the orthogonal projector with null space spanned by $\dot{\mathbf{x}}$. This equation is the geometric equation induced by generator $\ddot{\mathbf{x}} + \mathbf{M}_e^{-1} \mathbf{f}_e = \mathbf{0}$. Therefore, the energy equations of motion $\mathbf{M}_e \ddot{\mathbf{x}} + \mathbf{f}_e = \mathbf{0}$ form a geometric generator whose geometric equation is given by the geometric equations of motion $\mathbf{M}_g \ddot{\mathbf{x}} + \mathbf{f}_g = \mathbf{0}$. ■

The previous proof alluded to a number of properties of the generalized momentum $\mathbf{p}_e = \mathbf{M}_e \dot{\mathbf{x}}$ and energy \mathcal{L}_e . These are collected into the following Lemma and proved. These identities match the form seen in Riemannian geometry simply with the Riemannian metric replaced by the generalized metric tensor. See Section III-C for details.

Lemma III.2 (Energy and momentum identities). *Let \mathcal{L}_g be a Finsler structure with energy form $\mathcal{L}_e = \frac{1}{2} \mathcal{L}_g^2$, and denote the generalized momentum $\mathbf{p}_e = \partial_{\dot{\mathbf{x}}} \mathcal{L}_e$. Then*

$$1) \quad \mathbf{p}_e = \mathbf{M}_e \dot{\mathbf{x}}$$

$$2) \quad \mathcal{L}_e = \frac{1}{2} \mathbf{p}_e^T \dot{\mathbf{x}} = \frac{1}{2} \dot{\mathbf{x}}^T \mathbf{M}_e \dot{\mathbf{x}} = \frac{1}{2} \mathbf{p}_e^T \mathbf{M}_e^{-1} \mathbf{p}_e.$$

Proof. Since \mathcal{L}_e is homogeneous of degree 2, as we've seen $\mathcal{H}_{\mathcal{L}_e} = \mathbf{p}_e^T \dot{\mathbf{x}} - \mathcal{L}_e = \mathcal{L}_e$. This directly implies

$$\mathcal{L}_e = \frac{1}{2} \mathbf{p}_e^T \dot{\mathbf{x}} \quad (60)$$

giving the first form of identity (2). The rest of those identities derive from identity (1); to prove that identity, we take the gradient of this expression for \mathcal{L}_e

$$\partial_{\dot{\mathbf{x}}}\mathcal{L}_e + = \partial_{\dot{\mathbf{x}}}\left[\frac{1}{2}\partial_{xd}\mathcal{L}_e^T\dot{\mathbf{x}}\right] \quad (61)$$

$$= \frac{1}{2}\partial_{\dot{\mathbf{x}}}^2\mathcal{L}_e\dot{\mathbf{x}} + \frac{1}{2}\partial_{\dot{\mathbf{x}}}\mathcal{L}_e \quad (62)$$

which implies

$$\partial_{\dot{\mathbf{x}}}^2\mathcal{L}_e\dot{\mathbf{x}} = 2\partial_{\dot{\mathbf{x}}}\mathcal{L}_e - \partial_{\dot{\mathbf{x}}}\mathcal{L}_e = \partial_{\dot{\mathbf{x}}}\mathcal{L}_e \quad (63)$$

or $\mathbf{M}_e\dot{\mathbf{x}} = \mathbf{p}_e$. \blacksquare

C. Riemannian geometry is a Finsler geometry

Riemannian geometry is a special case of Finsler geometry. This section shows how the properties of Riemannian geometry arise from the more general properties of Finsler geometry. The Riemannian Finsler structure is $\mathcal{L}_g = (\dot{\mathbf{x}}^T\mathbf{G}(\mathbf{x})\dot{\mathbf{x}})^{\frac{1}{2}}$, where $\mathbf{G}(\mathbf{x})$ is a smoothly changing symmetric positive definite matrix. Since \mathbf{G} is independent of $\dot{\mathbf{x}}$, it's easy to see that the Finsler structure is HD1

$$\begin{aligned} \mathcal{L}_g(\mathbf{x}, \lambda\dot{\mathbf{x}}) &= ((\lambda\dot{\mathbf{x}})^T\mathbf{G}(\mathbf{x})(\lambda\dot{\mathbf{x}}))^{\frac{1}{2}} \\ &= (\lambda^2\dot{\mathbf{x}}^T\mathbf{G}(\mathbf{x})\dot{\mathbf{x}})^{\frac{1}{2}} \\ &= \lambda\mathcal{L}_g(\mathbf{x}, \dot{\mathbf{x}}). \end{aligned}$$

Likewise, since \mathbf{G} is positive definite $\mathcal{L}_g \geq \mathbf{0}$ with equality only when $\dot{\mathbf{x}} = \mathbf{0}$. And since $\mathcal{L}_e = \frac{1}{2}\dot{\mathbf{x}}^T\mathbf{G}\dot{\mathbf{x}}$, we have $\mathbf{M}_e = \partial_{\dot{\mathbf{x}}}^2\mathcal{L}_e = \mathbf{G}$, which is everywhere invertible. The matrix \mathbf{G} is called a *Riemannian metric*, and plays the role of the Finsler metric tensor. The Finsler structure defines a norm on the tangent space

$$\mathcal{L}_g = (\dot{\mathbf{x}}^T\mathbf{G}\dot{\mathbf{x}})^{\frac{1}{2}} = \|\dot{\mathbf{x}}\|_{\mathbf{G}}, \quad (64)$$

showing that the action defining the extremal problem's objective is

$$A[\mathbf{x}] = \int \mathcal{L}_g dt = \int \|\dot{\mathbf{x}}\|_{\mathbf{G}} dt, \quad (65)$$

can be understood as a generalized arc-length integral across the trajectory.

Since the action is a generalized arc-length integral it seems natural that this measure would be invariant to time-reparameterization of the trajectory (i.e. invariant to speed profile across the trajectory). Using time-reparameterization $t(s)$ with $\dot{\mathbf{x}}_s = \frac{dt}{ds}\dot{\mathbf{x}}_t$, we can perform the calculation of Section III-C

explicitly

$$\begin{aligned} A[\mathbf{x}_s] &= \int \|\dot{\mathbf{x}}_s\|_{\mathbf{G}} ds = \int \left\| \frac{dt}{ds} \dot{\mathbf{x}}_t \right\|_{\mathbf{G}} ds \\ &= \int \|\dot{\mathbf{x}}_t\|_{\mathbf{G}} \frac{dt}{ds} ds = \int \|\dot{\mathbf{x}}_t\|_{\mathbf{G}} dt = A[\mathbf{x}_t]. \end{aligned}$$

Per Theorem III.1 we would expect the Riemannian Finsler structure's Euler-Lagrange equation $\mathbf{M}_g\ddot{\mathbf{x}} + \mathbf{f}_g = \mathbf{0}$ to have a reduced rank $\mathbf{M}_g = \partial_{\dot{\mathbf{x}}}^2\mathcal{L}_g$ (otherwise, it would have a unique (non-redundant) solution). Indeed, by calculation, we have

$$\begin{aligned} \mathbf{M}_g &= \partial_{\dot{\mathbf{x}}}^2\mathcal{L}_g = \partial_{\dot{\mathbf{x}}}\left[\partial_{\dot{\mathbf{x}}}(\dot{\mathbf{x}}^T\mathbf{G}(\mathbf{x})\dot{\mathbf{x}})^{\frac{1}{2}}\right] \\ &= \partial_{\dot{\mathbf{x}}}\left[\frac{1}{2}(\dot{\mathbf{x}}^T\mathbf{G}\dot{\mathbf{x}})^{-\frac{1}{2}}2\mathbf{G}\dot{\mathbf{x}}\right] = \partial_{\dot{\mathbf{x}}}\left[\frac{\mathbf{G}\dot{\mathbf{x}}}{\|\dot{\mathbf{x}}\|_{\mathbf{G}}}\right] \\ &= \frac{\|\dot{\mathbf{x}}\|_{\mathbf{G}}\mathbf{G} - \mathbf{G}\dot{\mathbf{x}}\left(\frac{\dot{\mathbf{x}}^T\mathbf{G}}{\|\dot{\mathbf{x}}\|_{\mathbf{G}}}\right)}{\|\dot{\mathbf{x}}\|_{\mathbf{G}}^2} \\ &= \frac{1}{\|\dot{\mathbf{x}}\|_{\mathbf{G}}}\left[\mathbf{G} - \frac{\mathbf{G}\dot{\mathbf{x}}\dot{\mathbf{x}}^T\mathbf{G}}{\|\dot{\mathbf{x}}\|_{\mathbf{G}}}\right] \\ &= \frac{1}{\|\dot{\mathbf{x}}\|_{\mathbf{G}}}\mathbf{G}^{\frac{1}{2}}[\mathbf{I} - \hat{\mathbf{v}}\hat{\mathbf{v}}^T]\mathbf{G}^{\frac{1}{2}}, \end{aligned}$$

where $\hat{\mathbf{v}} = \mathbf{G}^{\frac{1}{2}}\dot{\mathbf{x}}$. This matrix is reduced rank since $\mathbf{I} - \hat{\mathbf{v}}\hat{\mathbf{v}}^T$ is an orthogonal projector (with null space spanned by $\hat{\mathbf{v}}$).

\mathbf{M}_g 's null space is, therefore, spanned by \mathbf{u} such that $\mathbf{G}^{\frac{1}{2}}\mathbf{u} = \mathbf{v} = \mathbf{G}^{\frac{1}{2}}\dot{\mathbf{x}}$. That means solutions to $\mathbf{M}_g\ddot{\mathbf{x}} + \mathbf{f}_g = \mathbf{0}$ can be expressed as any nominal solution $\ddot{\mathbf{x}}_0$ offset by a null space element $\alpha\dot{\mathbf{x}}$, i.e. $\ddot{\mathbf{x}} = \ddot{\mathbf{x}}_0 + \alpha\dot{\mathbf{x}}$.

Remember that Hamiltonian (conserved quantity) of the energy system defined by $\mathcal{L}_e = \frac{1}{2}\mathcal{L}_g^2$ is (generically) $\mathcal{H}_{\mathcal{L}_e} = \partial_{\dot{\mathbf{x}}}\mathcal{L}_e^T\dot{\mathbf{x}} - \mathcal{L}_e$. In the Riemannian case, this Hamiltonian is known to evaluate to

$$\mathcal{H}_{\mathcal{L}_e} = (\mathbf{G}\dot{\mathbf{x}})^T\dot{\mathbf{x}} - \frac{1}{2}\dot{\mathbf{x}}^T\mathbf{G}\dot{\mathbf{x}} = \frac{1}{2}\dot{\mathbf{x}}^T\mathbf{G}\dot{\mathbf{x}} = \mathcal{L}_e. \quad (66)$$

From the above discussion around homogeneous functions (see Section II) we know that this seemingly coincidental results actually derives from the second-degree homogeneity of \mathcal{L}_e , which in turn derives from the first-degree homogeneity of the Finsler structure $\mathcal{L}_g = (\dot{\mathbf{x}}^T\mathbf{G}(\mathbf{x})\dot{\mathbf{x}})^{\frac{1}{2}}$.

The energy equations $\mathbf{M}_e\ddot{\mathbf{x}} + \mathbf{f}_e = \mathbf{0}$ for the

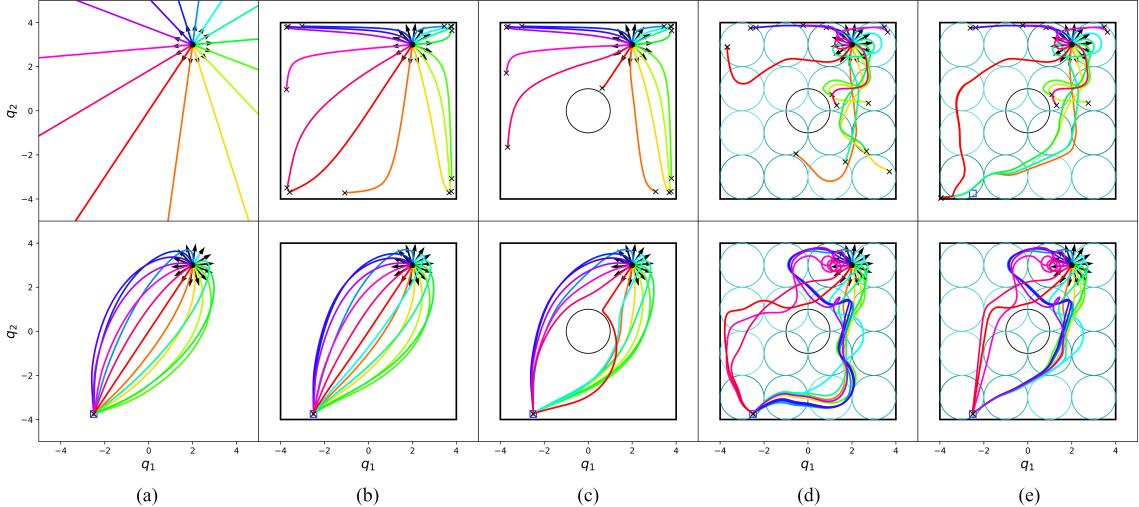


Fig. 3. Geometric fabrics, an application of general nonlinear and Finsler geometries for the modeling and design of reactive robotic behavior. Top row, a sophisticated geometry constructed layer-by-layer with increasing complexity from left-to-right. Bottom row, the resulting convergent system when forced by an objective potential. See Section IV for details.

Riemannian case have

$$\begin{aligned} \mathbf{M}_e &= \partial_{\dot{\mathbf{x}}}^2 \mathcal{L}_e = \mathbf{G} \\ \text{and } \mathbf{f}_e &= \partial_{\dot{\mathbf{x}}\dot{\mathbf{x}}} \mathcal{L}_e \dot{\mathbf{x}} - \partial_{\dot{\mathbf{x}}} \mathcal{L}_e \\ &= \partial_{\dot{\mathbf{x}}} (\mathbf{G} \dot{\mathbf{x}}) \dot{\mathbf{x}} - \partial_{\dot{\mathbf{x}}} \left(\frac{1}{2} \dot{\mathbf{x}}^T \mathbf{G} \dot{\mathbf{x}} \right). \end{aligned}$$

From these expressions we can easily see that \mathbf{M}_e is HD0 and \mathbf{f}_e is HD2, making $\ddot{\mathbf{x}} + \mathbf{M}_e^{-1} \mathbf{f}_e = \mathbf{0}$ an HD2 geometry generator. We do not fully derive the geometric equation here, but this result in conjunction with the above observation that \mathbf{M}_g is reduced rank support the results of Theorem III.1.

Finally, we note that there is a direct one-to-one correspondence between Riemannian geometry energy systems and classical mechanical systems, a formulation known as geometric mechanics [3]. Under this correspondence, $\mathbf{M}_e = \mathbf{G}$ is the generalized mass matrix and \mathbf{f}_e captures fictitious forces such as Coriolis and centripetal forces. The energy $\mathcal{L}_e = \frac{1}{2} \dot{\mathbf{x}}^T \mathbf{G} \dot{\mathbf{x}}$ is the kinetic energy of the mechanical system and the quantity $\mathbf{p}_e = \partial_{\dot{\mathbf{x}}} \mathcal{L}_e = \mathbf{G} \dot{\mathbf{x}}$ is the generalized momentum. These quantities match the generalized versions given by Lemma III.2.

System solutions of the generator $\mathbf{M}_e \ddot{\mathbf{x}} + \mathbf{f}_e = \mathbf{0}$ conserve the Hamiltonian and are, therefore, constant energy solutions and can be considered to be energy levels. Since $\mathbf{M}_e \ddot{\mathbf{x}} + \mathbf{f}_e = \mathbf{0}$ is a generator, the solutions are geometrically consistent (solutions of all initial value problems with initial velocity pointing in the same direction from the same initial

point follow overlapping paths).

IV. AN APPLICATION: GEOMETRIC FABRICS

These experiments show particle motion generated by optimizing a task space potential over an incrementally sequenced geometric fabric. Fourteen particles are created with initial conditions, $\mathbf{q}_0 = [2, 3]^T$ and $\|\dot{\mathbf{q}}_0\| = 1.5$, with headings radially distributed from 0 to 2π . Motion is integrated forward with the Runge-Kutta fourth-order routine for 16 s of simulation time. The sequential construction of the geometric fabric showcases how motion behavior can be incrementally modified while still guaranteeing optimization.

A. Task Space Potential

A potential for pulling the end-effector towards a target location is constructed with the task map is $\mathbf{x} = \phi(\mathbf{q}) = \mathbf{q} - \mathbf{q}_d$, where $\mathbf{q}, \mathbf{q}_d \in \mathbb{R}^2$ are the current and desired particle position in Euclidean space. The metric is designed as

$$\mathbf{G}_\psi(\mathbf{x}) = (\bar{m} - \underline{m}) e^{-(\alpha_m \|\mathbf{x}\|)^2} I + \underline{m} I. \quad (67)$$

where $\bar{m}, \underline{m} \in \mathbb{R}^+$ are the upper and lower isotropic masses, respectively, and $\alpha_m \in \mathbb{R}^+$ controls the width of the radial basis function. For the following experiments, $\bar{m} = 2$, $\underline{m} = 0.2$, and $\alpha_m = 0.75$. The acceleration-based potential gradient, $\partial_{\mathbf{q}} \psi(\mathbf{x}) = M_\psi(\mathbf{x}) \partial_{\mathbf{q}} \psi_1(\mathbf{x})$, is designed with

$$\psi_1(\mathbf{x}) = k \left(\|\mathbf{x}\| + \frac{1}{\alpha_\psi} \log(1 + e^{-2\alpha_\psi \|\mathbf{x}\|}) \right) \quad (68)$$

where $k \in \mathbb{R}^+$ controls the overall gradient strength, $\alpha_\psi \in \mathbb{R}^+$ controls the transition rate of $\partial_{\mathbf{q}}\psi_1(\mathbf{x})$ from a positive constant to 0. For these experiments, $k = 10$, $\alpha_\psi = 10$. A policy is constructed for this potential as $\dot{\mathbf{x}} = -\partial_{\mathbf{x}}\psi_1(\mathbf{x})$ and weighted by $\mathbf{M}_\psi(\mathbf{x})$ from the Finsler energy, $\mathcal{L} = \dot{\mathbf{x}}^T \mathbf{G}_\psi(\mathbf{x}) \dot{\mathbf{x}}$. For more information on prioritization and system damping, see [19].

B. Baseline Geometry

The baseline geometry is constructed from $\mathbf{h}_{2,b} = 0$ and prioritized with an energy tensor, M_b , from the Finsler energy, $\mathcal{L}_{e,b} = \frac{\lambda_b}{2} \mathbf{q}^T \mathbf{q}$, where $\lambda \in \mathbb{R}^+$ is a parameter that defines the amount of baseline inertia. For these experiments, $\lambda_b = 1$. The underlying geometry results in straight-line motion due to the nature of the Euclidean geometry (see first row in Figure 3a). Optimizing the task potential over this fabric results in a symmetric plume that terminates at the minimum of the potential (second row Figure 3a).

C. Coordinate Limit Avoidance

The distance to an upper and lower coordinate limit can be described as $x = \bar{q}_j - q_j$ and $x = q_j - \underline{q}_j$, respectively, where \bar{q}_j and \underline{q}_j are the upper and lower limits of the j^{th} coordinate of \mathbf{q} . Overall, $2n$ task maps, x , are needed for n -dimensional coordinates, \mathbf{q} . Repulsive geometries can be constructed in this one-dimensional space as $h_{2,i}(x, \dot{x}) = \lambda \dot{x}^2 \partial_x \psi(x)$, where the potential $\psi(x)$ is designed as,

$$\psi(x) = \frac{\alpha_1}{x^2} + \alpha_2 \log \left(e^{-\alpha_3(x-\alpha_4)} + 1 \right). \quad (69)$$

Moreover, $\alpha_1, \alpha_2 \in \mathbb{R}^+$ control the significance and mutual balance of the first and second terms. $\alpha_3 \in \mathbb{R}^+$ controls the sharpness of the smooth rectified linear unit (SmoothReLU) while α_4 offsets the SmoothReLU. For the following experiments, $\alpha_1 = 0.4$, $\alpha_2 = 0.2$, $\alpha_3 = 20$, and $\alpha_4 = 5$. The gradient of this potential is nearly constant away from coordinate limits, and unlimited as $x \rightarrow 0$.

To establish appropriate priorities for these geometries, individual energy tensors, M_i , are created from energies, \mathcal{L}_{e_i} , where $i = 1, \dots, 2n$. \mathcal{L}_{e_i} is designed as $\mathcal{L}_{e_i} = \frac{1}{2} s(\dot{x}) G(x) \dot{x}^2$. where the metric

is designed as $G(x) = \frac{\lambda}{x}$ and a switching function $s(\dot{x})$, where $s(\dot{x}) = 0$ if $\dot{x}(q_j) \geq 0$ and $s(\dot{x}) = 1$, otherwise. Effectively, this removes the effect of the coordinate limit geometry once motion is orthogonal or away from the limit. To illustrate the effect of adding this geometry to the system, limits are placed at ± 4 for both q_1 and q_2 , a two-dimensional Euclidean space. Furthermore, $\lambda = 0.25$. If particles are far away from their limits, then straight-line motion is observed due to the underlying Euclidean geometry. As particles approach limit boundaries, repulsion impedes motion towards the limits, and motion is ultimately redirected to limit corners before any one limit is reached (see second column of Fig. 3a). Optimization was conducted with this geometry included as can be seen in the second row of Fig. 3b. Importantly, behavior is not significantly influenced when motion is away from limits or distance to limits are larger. Subtle behavioral changes can be seen by the slight bulging of the particle plume and the approach to the target is slightly more aligned with the vertical direction.

D. Collision Avoidance

Collision avoidance with respect to a circular object is constructed as follows. The task map is $x = \phi(\mathbf{q}) = \frac{\|\mathbf{q} - \mathbf{q}_o\|}{r} - 1$, where \mathbf{q}_o is the origin of the circle and r is its radius. The geometry is $h_{2,o}(x, \dot{x}) = -s(\dot{x}) \dot{x}^2 \partial_x \psi(x)$, where $s(\dot{x})$ is the same as before and $\psi(x)$ is that in (69). The addition of this geometry further modifies the system's behavior as seen in the first row of Fig. 3c. During optimization, the effect from this geometry is significant in redirecting the paths around the obstacle while still minimizing the potential as seen in the second row of Fig. 3c

E. Vortices

Randomized vortex geometries are created as $\mathbf{h}_{2,j}(\mathbf{q}, \dot{\mathbf{q}}) = f_j \|\dot{\mathbf{q}}\|^2 \mathbf{R}_j \dot{\mathbf{q}}$, where $\mathbf{R}_j \in \mathbb{R}^{2 \times 2}$ is a rotation matrix randomly selected as either

$$\mathbf{R}_j = \pm \begin{bmatrix} 0 & -1 \\ 1 & 0 \end{bmatrix} \quad (70)$$

and $f \in \mathbb{R}^+$ is a force magnitude uniformly drawn from the interval $f \sim \mathcal{U}(2, 10)$. A radial priority for this geometry was created from the energy tensor of the following energy, $\mathcal{L}_{e,j} = ms(\mathbf{q}) \dot{\mathbf{q}}^T \dot{\mathbf{q}}$, where $m \in \mathbb{R}^+$ is a mass constant and the switching

function $s(\mathbf{q}) \in [0, 1]$ is defined as

$$s(\mathbf{q}) = \begin{cases} \frac{1}{\|\mathbf{q} - \mathbf{q}_{o,j}\|^2} (\|\mathbf{q} - \mathbf{q}_{o,j}\| - r)^2 & \|\mathbf{q} - \mathbf{q}_{o,j}\| < r \\ 0 & \text{otherwise} \end{cases} \quad (71)$$

where $\mathbf{q}_{o,j}$ is the effect center of a vortex and $r \in \mathbb{R}^+$ is its radius. In these experiments, $r = 1$ for all vortices. The addition of this geometry significantly redirects the paths of the particles as they move through the circular regions of vortices. Despite this rather chaotic behavior, the system still optimizes while under significant influence of these vortices (see Fig. 3d).

F. Point Attraction

Finally, a point attraction geometry is created as $\mathbf{h}_{2,a} = \lambda_a \|\dot{\mathbf{q}}\|^2 \partial_{\mathbf{q}} \psi(\phi(\mathbf{q}))$, where $\lambda_a \in \mathbb{R}^+$ is a control gain. This geometry is prioritized with the energy tensor from the energy, $\mathcal{L}_e, a = \dot{\mathbf{x}}^T \mathbf{G}_a \dot{\mathbf{x}}$, where the metric \mathbf{G}_a is designed as $\mathbf{G}_a = s(\mathbf{x})(\bar{m} - \underline{m})I + \underline{m}I$, where \bar{m} and \underline{m} are the upper and lower isotropic mass values and the switching function is designed as $s(\mathbf{x}) = \frac{1}{2}(\tanh(-\alpha_s(\|\mathbf{x}\| - r)) + 1)$, where $\alpha_s \in \mathbb{R}^+$ controls the rate of the switch and r is the effect radius. Overall, this metric allows the priority to transition from a small to a large isotropic priority as the position nears the target. For these experiments, $\bar{m} = 1$, $\underline{m} = 0$, $\alpha_s = 25$, $r = 5$, $\lambda_a = 7$. The parameter values for the attracting potential from Equation 68 are $k = 1$ and $\alpha_\psi = 1$. Effectively, this geometry does not engage until the Euclidean distance between the current position and the target is within 5 units. The addition of this geometry redirects motion towards the target location and which can also facilitate optimization as shown in Fig. 3e.

V. SUMMARY

We've presented the fundamentals of generalized nonlinear geometries, characterized by HD2 second-order differential equations, and Finsler geometries, defined by a special type of *geometric* Lagrangian known as a Finsler structure that defines a velocity-dependent *length element* for defining geodesics using the Calculus of Variations. While the latter is derived using the Euler-Lagrange equation, we see in Theorem III.1 that the resulting equations define generalized nonlinear geometries in the same sense as defined in Section II. All of these generalized geometries, therefore, exhibit a form of

path-consistency enabling us to characterize them as nonlinear geometries of paths.

We saw that Finsler geometries naturally generalize Riemannian geometry to the case where the metric tensor can take on a velocity dependence (the amount by which the space is stretched in any given direction is dependent on the heading of the system). And each Finsler geometry corresponds to a dynamical system (derived using the Euler-Lagrange equation applied to its energy form) in the same way each Riemannian geometric system corresponds to a classical mechanical system (an observation studied under geometric mechanics [3]). All such Finsler dynamical systems defined by a Finsler energy $\mathcal{L}_e = \frac{1}{2}\mathcal{L}_g^2$ from Finsler structure \mathcal{L}_g exhibit conserved energy \mathcal{L}_e , have directionally dependent mass $\mathbf{M}_e = \partial^2 \dot{\mathbf{x}} \mathcal{L}_e$ defined its *energy tensor*, and have momentum expressions analogous to the classical setting $\mathbf{p}_e = \partial_{\dot{\mathbf{x}}} \mathcal{L}_e^T \dot{\mathbf{x}} = \mathbf{M}_e \dot{\mathbf{x}}$ and $\mathcal{L}_e = \frac{1}{2}\mathcal{L}_g^2 = \frac{1}{2}\mathbf{p}_e^T \mathbf{M}_e^{-1} \mathbf{p}_e = \frac{1}{2}\dot{\mathbf{x}}^T \mathbf{M}_e \dot{\mathbf{x}}$ (see Lemma III.2).

These geometries have already been fundamental to the development of our theory of Geometric Fabrics [9] which have produced the most flexible, intuitive, consistent, and provably stable tools to date for the modular design of reactive robot behavior. It is our hope that this more accessible presentation of the underlying mathematics and properties of generalized nonlinear and Finsler geometries will additionally inspire new varied and creative applications of the material within the robotics community.

REFERENCES

- [1] N. D. Ratliff, K. V. Wyk, M. Xie, A. Li, and A. M. Rana, “Generalized nonlinear and finsler geometry for robotics,” *arXiv preprint arXiv:(in prep)*, 2020.
- [2] R. M. Murray, Z. Li, and S. S. Sastry, *A Mathematical Introduction to Robotic Manipulation*. CRC Press, 1994.
- [3] F. Bullo and A. D. Lewis, *Geometric control of mechanical systems: modeling, analysis, and design for simple mechanical control systems*. Springer Science & Business Media, 2004, vol. 49.
- [4] N. D. Ratliff, J. Issac, D. Kappler, S. Birchfield, and D. Fox, “Riemannian motion policies,” *arXiv preprint arXiv:1801.02854*, 2018.
- [5] N. Ratliff, M. Toussaint, and S. Schaal, “Understanding the geometry of workspace obstacles in motion optimization,” in *IEEE International Conference on Robotics and Automation (ICRA)*, 2015.
- [6] C.-A. Cheng, M. Mukadam, J. Issac, S. Birchfield, D. Fox, B. Boots, and N. Ratliff, “RMPflow: A computational graph for automatic motion policy generation,” in *The 13th International Workshop on the Algorithmic Foundations of Robotics*, 2018.
- [7] G. B. Folland, *Advanced Calculus*. Pearson; 1st Edition, 2001.
- [8] I. Gelfand and S. Fomin, *Calculus of Variations*. Dover, orig. Prentice-Hall, 1963.
- [9] M. Xie, K. V. Wyk, A. Li, M. A. Rana, D. Fox, B. Boots, and N. Ratliff, “Geometric fabrics for the acceleration based design of robotic motion,” *arXiv preprint arXiv:(in prep)*, 2020.
- [10] D. D.-W. Bao, S.-S. Chern, and Z. Shen, *An Introduction to Riemann-Finsler Geometry*. Springer; 2000th Edition, 2000.
- [11] Z. Shen, *Differential Geometry of Spray and Finsler Spaces*. Springer; 2001 Edition, 2001.
- [12] P.-A. Absil, R. Mahony, and R. Sepulchre, *Optimization Algorithms on Matrix Manifolds*. Princeton University Press, 2008.
- [13] J. R. Taylor, *Classical Mechanics*. University Science Books, 2005.
- [14] F. E. Udwadia and R. E. Kalaba, *Analytical Dynamics: A New Approach*. Cambridge University Press, 1996.
- [15] J. M. Lee, *Riemannian Manifolds: An Introduction To Curvature*. Springer, 1997.
- [16] S. Carroll, *Spacetime and Geometry: An Introduction to General Relativity*. Pearson, 2003.
- [17] J. Lewis, *Homogeneous Functions and Euler’s Theorem*. In: *An Introduction to Mathematics*. Palgrave Macmillan, London., 1969.
- [18] J. M. Lee, *Introduction to Smooth Manifolds*, 2nd ed. Springer, 2012.
- [19] N. D. Ratliff, K. V. Wyk, M. Xie, A. Li, and A. M. Rana, “Generalized nonlinear and finsler geometry for robotics,” *arXiv preprint arXiv:(in prep)*, 2020.